Article

Pressure-Modulated Dissolution Behavior of LLM-105 Crystals in High-Temperature Water

Junke Wang,* Xiaoyu Sun,* Chan Gao, Zilong Xu, Di Mai, Rucheng Dai,* Zhongping Wang, Hongzhen Li, and Zengming Zhang*

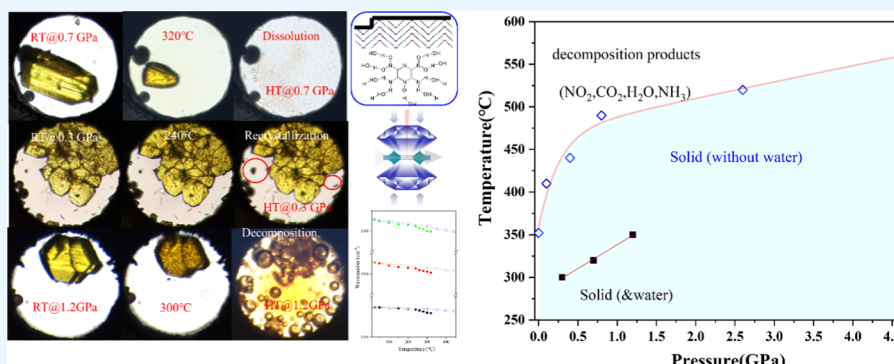Cite This: ACS Omega 2023, 8, 24654−24662

Read Online

ACCESS | Metrics & More | Article Recommendations | Supporting Information

ABSTRACT: The exploration of the microstructural evolution and reaction kinetics of energetic materials with high-temperature and high-pressure water contributes to the understanding of their microscopic physicochemical origin, which can provide critical experimental data for the use of energetic materials. As a promising high-energy and insensitive energetic material, LLM-105 has been investigated under extreme conditions such as high pressure and high temperature. However, little information is available about the effect of water on LLM-105 under high pressure and high temperature. In this work, the interaction between LLM-105 and water under HP-HT was investigated in detail. As a result, the dissolving behavior of LLM-105 in water under high pressure and high temperature is related to the initial pressure. When the initial pressure is less than 1 GPa, LLM-105 crystals are dissolved in high-temperature water; when the initial pressure is above 1 GPa, LLM-105 particles are only decomposed in high-temperature water. When the solution is saturated at a high temperature, recrystallization of the LLM-105 sample appears in the solution. High pressure hindered the dissolution process of the sample in HP-HT water because the interaction between the solute and the solvent was weakened by high pressure. The initial pressure is one of the significant parameters that determines whether LLM-105 crystals can be dissolved in high-temperature water. More importantly, water under high pressure and high temperature can not only act as a solvent when dissolving the samples but also act as a catalyst to accelerate the decomposition process. In addition, the HP-HT water reduced the decomposition temperature of the LLM-105 crystal to a large extent. The research in this paper not only provides insights into the interaction between LLM-105 and water but also contributes to the performance of energetic materials under extreme conditions and their practical applications in complex conditions.

1. INTRODUCTION

Water is a common solvent, but many organic materials hardly dissolve in ambient liquid water. On the other hand, water tends to become a weakly polar solvent with increasing temperature and pressure, so some organic materials, such as wood, willow, cellulose, and polyethylene terephthalate, possess high solubilities in HP-HT water.[1−8]

Generally, explosives undergo a series of extreme conditions, such as high pressure and high temperature, during detonation. Many explosives generate intermediate water and the final product of water in the process of decomposition. Some works have investigated the role of water from the decomposing product during detonation by experiments and calculations. Wu et al. found that water may catalyze complex explosive

reactions in the decomposition process of PETN, which is contrary to a previous work showing that water is simply a stable detonation product.[9] Additionally, He and Chen et al. tracked the dissociation process of HMX and discovered the special catalytic action of intermediate water.[10] The intermediate water catalyzes decomposition by affecting the
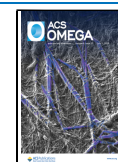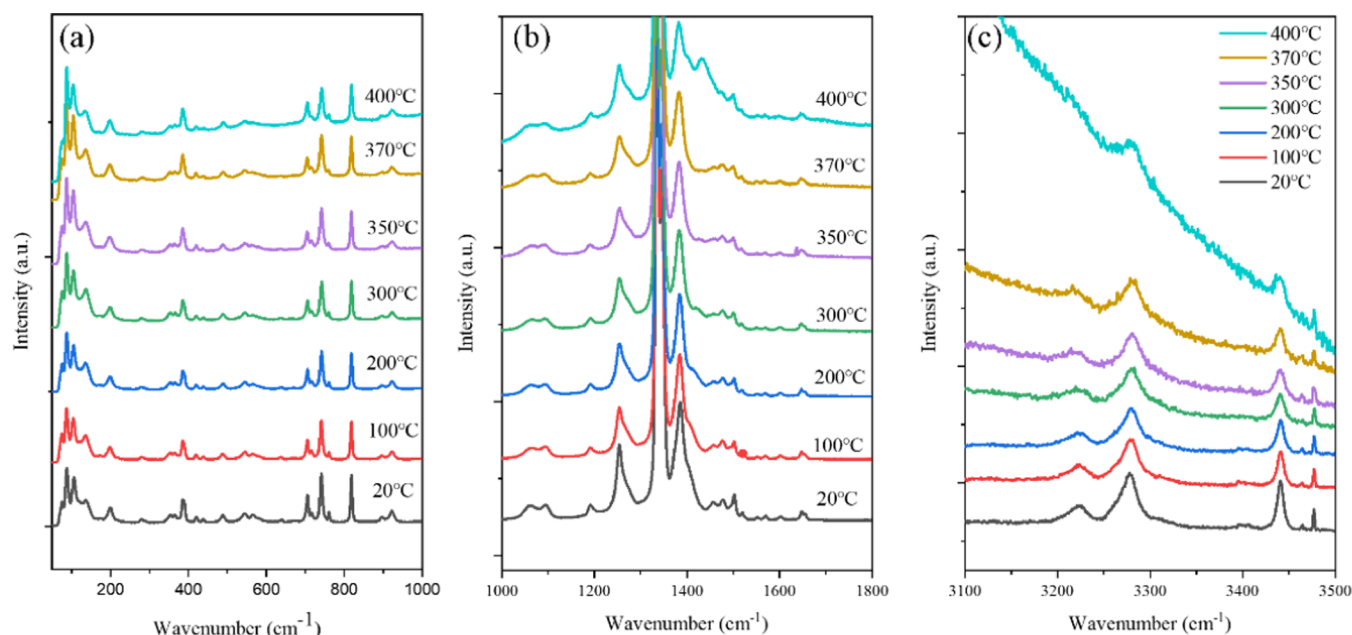
Figure 1. Temperature-dependent Raman spectra of the LLM-105 crystal without water with an initial pressure of 0.7 GPa. Raman spectra in the ranges of (a) $50-1000$ cm^{-1}, (b) $1000-1800$ cm^{-1}, and (c) $3100-3500$ cm^{-1}.

transport of oxygen, proton, and hydroxyl groups. However, the interactions between high-temperature high-pressure (HP-HT) water and energetic materials still remain insufficient.

2,6-Diamino-3,5-dinitropyrazine-1-oxide, known as LLM-105, is a typical nitro energetic material with some excellent properties, such as low sensitivity and high energy density.[11−20] The density of LLM-105 crystals is 1.919 g/cm^3 under ambient conditions, and the calculated energy content of LLM-105 is approximately 85% that of HMX.[20] The higher nitrogen content and density of LLM-105 lead to a higher detonation heat of 3.721 kJ/g, detonation velocity higher than 7.5 km/s, and detonation pressure higher than 30 GPa.[21] It possesses a monoclinic structure (space group $P21/n(14)$) with a wavelike $\pi-\pi$ stacking packing arrangement, which has four molecules in the unit cell, as presented in Figure S1a. In addition, each molecule consists of one pyrazine ring, two amino groups, two nitro groups, and one exposed oxygen atom.[22−25] Moreover, extensive intra- and intermolecular hydrogen-bond interactions exist in the LLM-105 crystal and maintain its structural stability up to 615 K at ambient pressure.[26−28]

For the LLM-105 explosive, extensive research has focused on the mechanism and the products of thermal decomposition.[29−31] Xiao et al. studied the gas release mechanism with three stages for LLM-105 at different temperatures by infrared spectroscopy.[29] Yu et al. investigated the mechanism of the two-step thermal decomposition for LLM-105.[31] In our previous works, we investigated the initial decomposition of LLM-105 under high temperature (HT) and/or high pressure (HP) and found that the reversibility of intramolecular H transfer is responsible for the low sensitivity mechanism of LLM-105.[32,33] The results indicated that the initial decomposition mechanism varies under high pressure and high temperature.

These investigations mentioned the role of water in the products during the thermal decomposition of the explosives. As described above, these products and raw explosives should undergo a high-pressure and high-temperature environment. In the process of detonation, transport, and storage, explosives

should exist in a small amount of water under high pressure and high temperature. The dissolution evolution of explosives in water under high pressure and high temperature can help us understand the explosive performance in water.

In previous thermal decomposition investigations of LLM-105, H$_2$O was one of the main decomposition products. H$_2$O, as an intermediate and/or final product, should modify the reaction progress of LLM-105 under HP and HT. However, very little information is available about the solubility evolution of energetic materials in water under HP and HT. In the current work, the solubility evolution of LLM-105 crystals in water under high pressure and high temperature is investigated by microscopy, Raman spectroscopy, and IR spectroscopy. The results provide deep insights into the dissolving properties of organic energetic materials in water under high pressure and high temperature.

2. EXPERIMENTAL SECTION

LLM-105 crystals from the China Academy of Engineering Physics were prepared by the reported method and used without further purification.[26,27] A diamond anvil cell (DAC) with heaters was employed to generate the high-pressure and high-temperature environment. The diameter of the diamond culet was 400 μm, and a hole was drilled in a stainless-steel gasket with a diameter of 200 μm. The pressure calibration was determined by the R1 line of ruby luminescence.[34] A resistive heater wrapped around the diamond was used to control the temperature of the DAC, and the accuracy of the temperature was estimated to be 1 K. A K-type thermocouple was used to measure the temperature. The heating rate was kept at 3 k/min during all of the experiments. In the high-temperature high-pressure experiment, the LLM-105 crystal, ruby, and distilled deionized water were packed into the sample chamber. After preparing the sample and water in the DAC, the pressure was loaded first, and then, the temperature was increased to the set point.

The Raman spectra were obtained through a micro Raman system (HR800, JY-Horiba) equipped with a confocal
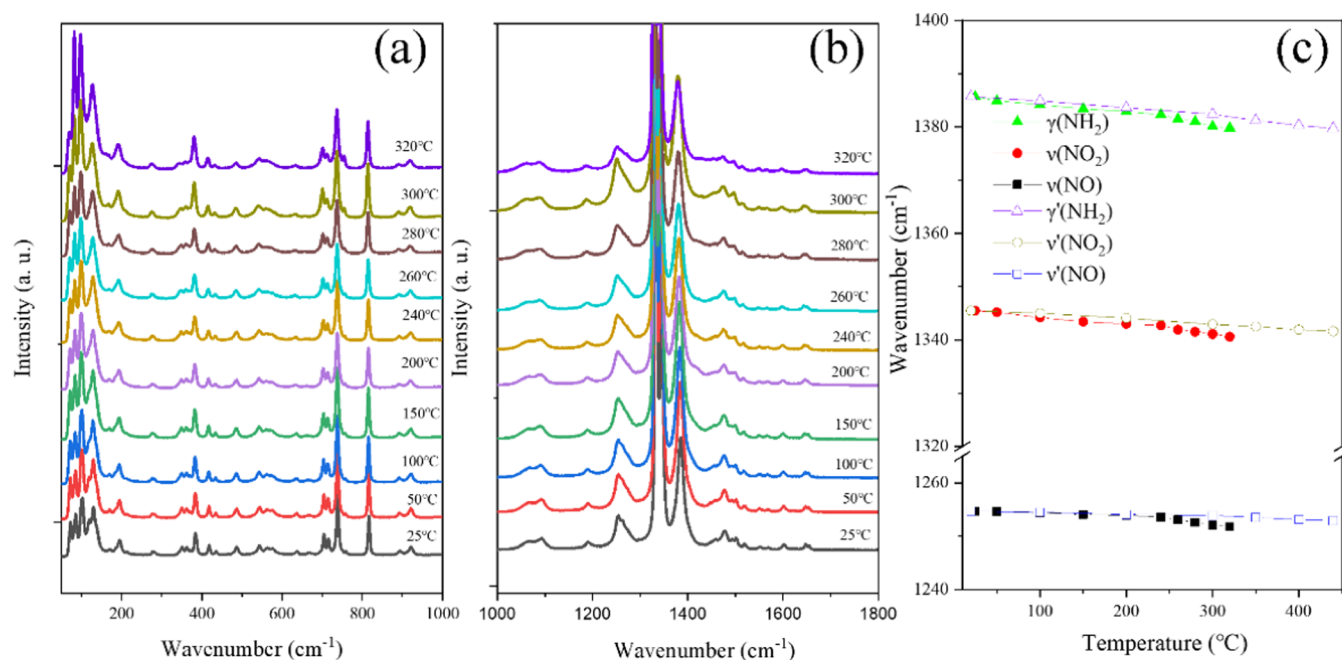
Figure 2. (a, b) Raman spectra of the LLM-105 crystal in water with an initial pressure of 0.7 GPa at different temperatures. (c) Temperature-dependent Raman shifts for the modes involving hydrogen bonds for LLM-105 crystals with/without water at an onset pressure of 0.7 GPa. The modes for the sample in water are labeled $\gamma(NH_2)$, $\nu(NO_2)$, and $\nu(NO)$, and the modes for the sample without water are $\gamma'(NH_2)$, $\nu'(NO_2)$, and $\nu'(NO)$. The modes of $\gamma(NH_2)$ and $\gamma'(NH_2)$ represent the rocking vibrations of NH$_2$ groups; the $\nu(NO_2)$ and $\nu'(NO_2)$ modes correspond to the symmetric stretching vibrations of nitro groups; and the $\nu(NO)$ and $\nu'(NO)$ modes correspond to the stretching vibrations of the $O-N_{in-ring}$ bond.
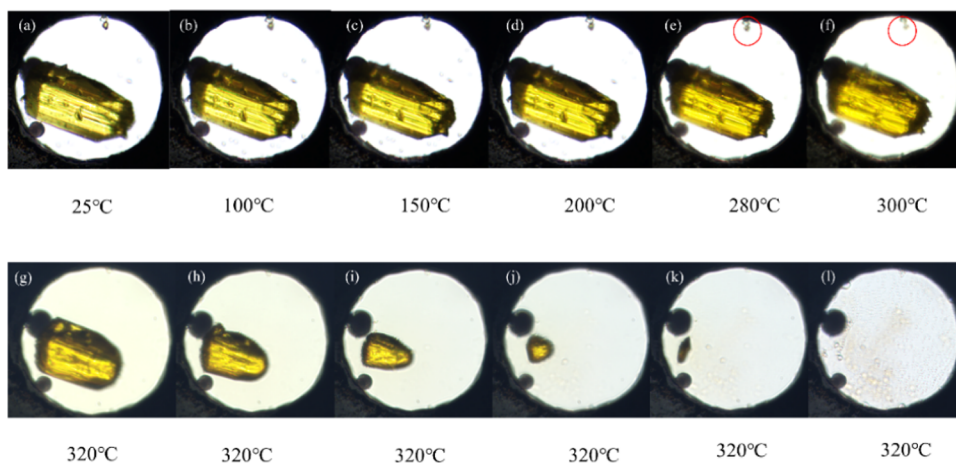

Figure 3. Optical microimages of the sample in water under high temperature with an initial pressure of 0.7 GPa. (a−g) With a heating rate of 3 k/min, (g−l) with a duration of 12 min for the chamber held at 320 °C.

microscope, a stigmatic spectrometer, and a multichannel air-cooled CCD detector. A 632.8 nm He-Ne laser was employed for excitation of the sample. The focal spot of a laser beam on the sample was around 20 μm. To reduce the fluorescence background and avoid damage to the sample, the incident power on the sample was controlled below 20 mW. During the heating process, in situ Raman spectra were measured, and optical micrographs were obtained.

3. RESULTS AND DISCUSSION

3.1. Stabilities of LLM-105 Crystals with/without Water at an Onset Pressure of 0.7 GPa with Increasing Temperature. The XRD pattern in Figure S1b exhibits diffraction peaks in accordance with the monoclinic crystal, suggesting the pure phase of LLM-105. The Raman and IR

spectra of the crystal under ambient conditions agree well with those previously reported for samples of LLM-105, as shown in Figure S2. Figure 1 shows the temperature-dependent Raman spectra of LLM-105 crystals without water at a primitive pressure of 0.7 GPa. There are no apparent changes except for Raman peak shifting and broadening for LLM-105 crystals up to 400 °C, as shown in Figure 1. In our previous work, we demonstrated that the decomposition temperature is greatly enhanced when the initial pressure is less than 1 GPa due to the pressure-induced strengthening of the hydrogen-bond network. The decomposition temperature of the LLM-105 crystal increases to 470 °C for an initial pressure of 0.7 GPa from 352 °C at ambient pressure.[13,33] However, the water may decrease the decomposition temperature to a large extent under HP-HT conditions.
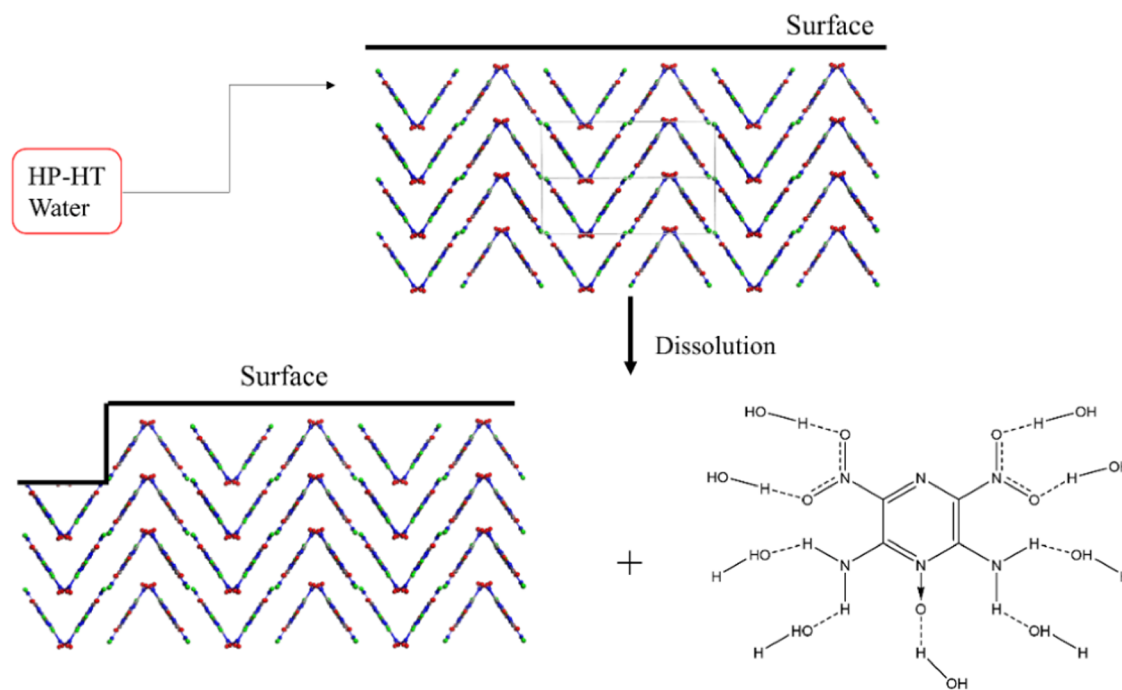
Figure 4. Schematic diagram of the dissolution behavior of LLM-105 in HP-HT water. The NO_2 group and the O atom bonding with the N atom in the ring can form intermolecular hydrogen bonds with nearby water molecules. When the interactions between molecules from the surface area of the LLM-105 crystal and HP-HT water are strong enough, the LLM-105 molecule can be dragged out and then form a water solution. When the temperature increases, the dielectric constant of water decreases and can act as a solvent. The distance between molecules shortened under high pressure, which enhanced the hydrogen-bond interaction between water and LLM-105 molecules.

Temperature-dependent Raman spectra of LLM-105 in water with an onset pressure of 0.7 GPa are displayed in Figure 2a,b. As the temperature increases, the Raman peaks also broaden and move to low frequencies below the dissolution temperature. At 320 °C, the LLM-105 crystal gradually dissolved into the water, as observed in the micrographs of Figure 3. During dissolution, the Raman spectra of the LLM-105 crystal maintain consistency with each other, as shown in Figure S3. After the LLM-105 crystal was completely dissolved, there was no signal relative to the LLM-105 crystal in the Raman spectrum. The results show the decomposition temperature in water is much lower than that without water under HP-HT, which demonstrates the catalyst behavior of HP-HT water.

As mentioned above, the pressure-induced hydrogen-bond enhancement lifts the decomposition temperature for the LLM-105 crystal without water. Although LLM-105 crystals are insoluble in water under ambient conditions, they can be soluble in water under high temperature and high pressure. The existence of water modifies the structural evolution pathway of the LLM-105 crystal under high temperature and high pressure.

Figure 2c compares the Raman shifts involving hydrogen bonds for LLM-105 without and with water under HP-HT conditions. At room temperature, the 1385 cm^{-1} peak is ascribed to the rocking vibration of the NH_2 group ($\gamma(NH_2)$), and the modes at 1350 and 1254 cm^{-1} correspond to the stretching vibrations of NO_2 groups and the stretching vibrations of the O−N$_{ring}$ bond, where the N atom is embedded in the ring. The peaks of $\gamma(NH_2)$, $\nu(NO_2)$, and $\nu(NO)$ are the Raman shifts of the crystal in water, while the peaks of $\gamma'(NH_2)$, $\nu'(NO_2)$, and $\nu'(NO)$ are from the sample without water. Three peaks of $\gamma'(NH_2)$, $\nu'_s(NO_2)$, and

$\nu'(NO)$ linearly shift to red with increasing temperature for water-free LLM-105, as shown in Figure 2c. Three peaks of $\gamma(NH_2)$, $\nu(NO_2)$, and $\nu(NO)$ maintain the sample red-shift rate below 240 °C and then accelerate the red-shift speed.

The same phenomena can be found, and the inflective point is approximately 200 °C for LLM-105 with water at an initial pressure of 0.3 GPa, as shown in Figure S4. First, heating improves the solubility of LLM-105 crystals in water under high pressure due to the properties of HP-HT water, which can also be found in other organic materials.[1−8] This is because water near its critical point (374 °C, 218 atm) possesses properties very different from those of ambient liquid water.[35−38] Water as a polar solvent under ambient conditions transfers to a weakly polar solvent due to the decreasing dielectric constant with increasing temperature under high pressure. The weakly polar solvent can dissolve some organic compounds, such as DAAF[39,40] and LLM-105. Therefore, the inflection points of 200 and 240 °C correspond to the initial soluble temperatures for LLM-105 crystals at the onset pressures of 0.3 and 0.7 GPa, respectively.

Figure 3 presents the optical micrograph of the sample in water under high temperature and high pressure. The heating rate was 3 K per minute. Some small LLM-105 particles initially dissolve in water at 280 °C for an onset pressure of 0.7 GPa, as indicated by the red circle labeled in the upper part of Figure 3e,f. The small particles at the upper corner from Figure 3e,f disappear at 320 °C, and the large particles enhance their transparency due to the dissolution of the cover tiny particles at approximately 300 °C. Holding the sample at 320 °C, the large crystal particle attenuates its size and completely dissolves after 12 min, as shown in Figure 3l. The optical micrograph shows that the initial soluble temperature is 280 °C higher than the value obtained from the Raman shift, as shown in
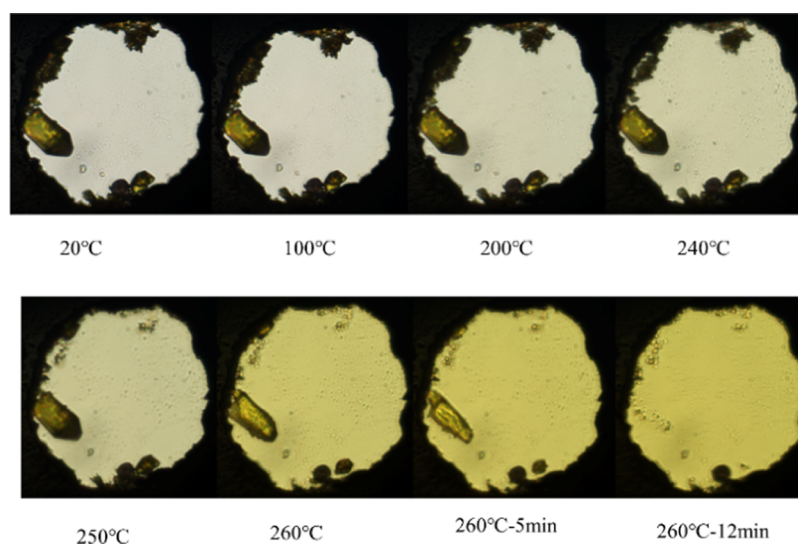
Figure 5. Micrographs of the LLM-105 sample in water with increasing temperature and an initial pressure of 0.3 GPa.
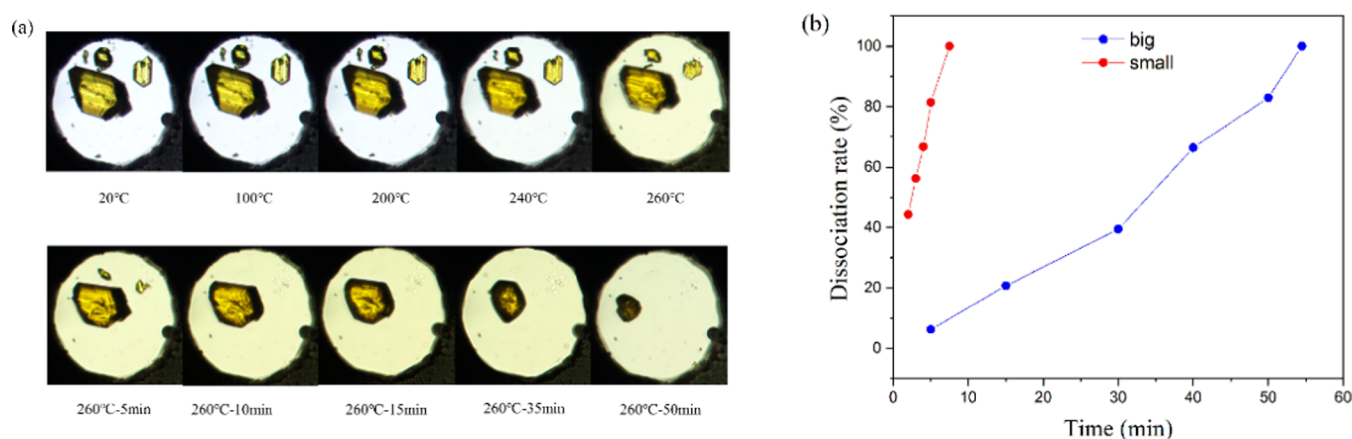

Figure 6. (a) Micrographs of LLM-105 particles with different sizes and an initial pressure of 0.3 GPa at different temperatures. (b) Dissociation rate of the largest particle and the smallest particle at 260 °C with an initial pressure of 0.3 GPa.

Figure 2. This demonstrates that Raman spectroscopy is more sensitive for detecting the primitive soluble temperature.

3.2. Dissolution Mechanism of LLM-105 Crystals in Water under High Pressure and High Temperature. The possible initial steps of molecular dissociation for the LLM-105 crystal in water are illustrated in Figure 4. The NO_2 group and the O atom bonding with the N atom in the ring can form intermolecular hydrogen bonds with nearby water molecules. When interactions such as hydrogen bonding between molecules from the surface area of the LLM-105 crystal and HP-HT water are strong enough, the LLM-105 molecule can be dragged out and then form a water solution. When the temperature increases, the dielectric constant of water decreases and can act as a solvent. The distance between molecules is shortened under high pressure, which enhances the hydrogen-bond interaction between water and LLM-105 molecules.

The variation in hydrogen-bond interactions between the LLM-105 molecule and H_2O molecules can also be seen from the Raman spectra, as displayed in Figure 2c. Above 240 °C with an initial pressure of 0.7 GPa, the enhanced hydrogen-bond networks constrict the vibrations involving the nitro and amino groups and result in the fast red-shift of the modes connected to these groups. Below 240 °C, few hydrogen bonds

hardly suppress the vibrations for these modes, so the red-shift rates are the same as those of LLM-105 without water, as shown in Figure 2c. HP-HT water dissolves LLM-105 molecules from the surface of the crystal, and then, the disengaged molecules diffuse into water. As observed in Figure 3, the dissolution is along the edges of the original crystals. This can also be speculated from the fact that small particles are easier to dissolve in HP-HT water, which will be discussed in the next section. With increasing separation of molecules cleaved from the crystal surface, the dissolved molecules further diffuse into the water, and finally, the solution saturates for the low ratio of LLM-105 particles in the chamber or the sample completely dissolves for the large ratio of water in the hole.

3.3. Saturated Dissolution and Particle Size-Dependent Dissolving Rate for LLM-105 Crystals in Water at an Initial Pressure of 0.3 GPa with Increasing Temperature. Figure 5 shows the temperature-dependent micrographs for LLM-105 crystals with water at an initial pressure of 0.3 GPa. These images reveal that the LLM-105 crystals initially dissolve at 260 °C and completely dissolve after 12 min at 260 °C. With the increasing dissolution of LLM-105 crystals, the color of the solution deepened slowly. After cooling the solution to room temperature, there were no
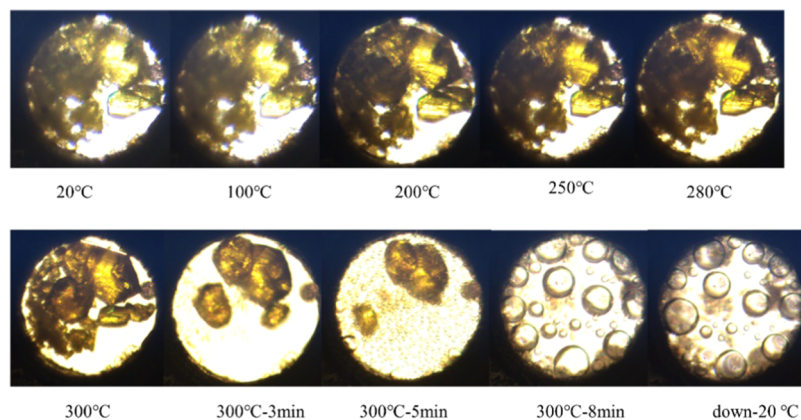
Figure 7. Optical micrographs of LLM-105 with increasing temperature. The initial pressure is 0.3 GPa. The sample occupying a large part of the hole begins to decompose as the solution reaches saturation when kept at high temperatures.
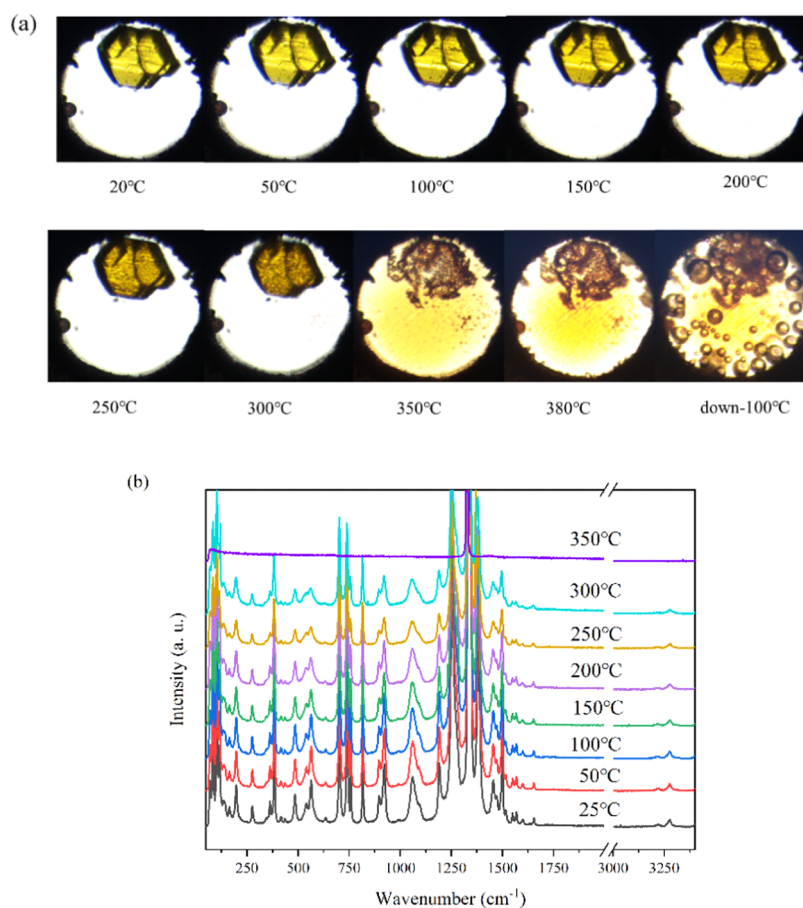

Figure 8. (a) Optical images of the sample in high-temperature water with an initial pressure of 1.2 GPa. (b) Raman spectra of LLM-105 during the heating process.

significant changes, and no recrystallization was observed after standing for several days. In the heating process, no obvious changes were found in the Raman spectra of LLM-105 crystals below the dissolution temperature of 260 °C, as shown in Figure S6. The Raman spectra of the solution at 260 °C and back to room temperature display no signal relative to LLM-105 crystals. The pressure in the chamber increases with increasing temperature, as shown in Figure S5.

As described above, particle size is an important parameter for solubility. In Figure 6, we compare the large particles and small particles of the LLM-105 powder crystals under HP-HT

with an initial pressure of 0.3 GPa. There are three particles of LLM-105 crystals in the chamber, and the smallest particle is dissolved first. The dissociation rates of the largest and smallest particles are shown in Figure 6b. The smaller particles dissolve faster than the larger crystals because they have a larger surface-to-volume ratio. Figure 4 is a schematic diagram of the dissolving mechanism for LLM-105 crystals in water under high pressure and high temperature. It is clear that LLM-105 molecules in the interface area of the crystal are first dissolved. Moreover, small particles possess a high specific surface area, so they contact HP-HT water and can be dissolved directly.

This process can be found in Figure S7. With an initial pressure of 0.3 GPa, the powder crystals occupy the majority of the DAC chamber. As the temperature increased, the small particles dissolved first, and the solution reached saturation. Finally, the remaining larger particles became transparent.

As shown in Figure S8, when the solution saturates under high temperature, small rodlike crystal particles of LLM-105 occur from the solution while maintaining the temperature at 260 °C. As shown by the red circle-labeled particles in Figure S8, the crystal size becomes larger after 30 min in the solution. It is comprehensible that the recrystallization of the LLM-105 sample would appear when the solution is saturated at high temperatures.

Figure 7 displays the evolution process of LLM-105 crystals in water at an initial pressure of 0.3 GPa with increasing temperature, where the ratio of water to sample is approximately 1:3. When the sample particles occupied the majority of the chamber, the sample dissolved partially as the temperature increased to 300 °C. The sample would not continue to dissolve due to rapid saturation. Holding the sample at 300 °C, the remaining crystals began to decompose. This indicates that the HP-HT water can not only dissolve the organic sample but also catalyze the decomposition process. The sample was completely decomposed after 8 min. The larger amount of gas products generates abundant bubbles in the chamber, as shown in Figure 7.

3.4. Repression of Dissolution of LLM-105 Crystals in Water under High Temperature and Pressure above 1 GPa.
The abovementioned initial pressure is limited below 1.0 GPa, and the LLM-105 crystal can dissolve in HP-HT water. In addition, experiments with an initial pressure above 1.0 GPa were carried out as well. The LLM-105 crystals with an initial pressure of 1.2 GPa are not dissolved below 300 °C and decompose above 350 °C, as shown in Figure 8a. The surface of the crystal becomes rough at 300 °C. The decomposition process was basically complete when the temperature was increased to 380 °C. As the temperature cools down to room temperature, bubbles start to appear in the chamber. Under high temperature and high pressure, the gases are miscible[35,38] in water, which leads to a few bubbles. The pressure in the sample chamber decreases with cooling, as shown in Figure S5. The lowering pressure results in the weak solubility of gas products in water and blows the bubbles, as shown in Figure 8a.

After complete decomposition, the residual black matter is presumed to be decomposition products such as carbon clusters. The Raman spectra during the heating process are illustrated in Figure 8b. Similar to the results of the initial pressure below 1 GPa, the Raman signal was almost unchanged except for the peak shifts and broadening before decomposition of the crystal. At 350 °C, the remaining products were measured by Raman spectroscopy, and there was no signal relative to the LLM-105 crystal.

Although the LLM-105 crystals occupy a very small rate relative to water in the sample chamber, they do not dissolve in water at an initial pressure above 1 GPa, which is totally different from the situation when the initial pressure is less than 1.0 GPa. After repeating the HP-HT experiments for LLM-105 in water several times, we concluded that the initial pressure is one of the significant parameters that determines whether LLM-105 can be dissolved in high-temperature water.

As the pressure increased, the diffusion of the solution was restricted, and then, the surface of the LLM-105 crystal was surrounded by the solution, thus making the contact area between the solute and solvent small. As a result, the whole dissolution process of the sample was repressed by high pressure. Finally, the crystal is decomposed with increasing temperature. In this case, HP-HT water only acts as a catalyst during the decomposition of the organic crystal.

Figure 9 shows a comparison of the pressure−temperature boundaries of the LLM-105 crystal under high pressure with
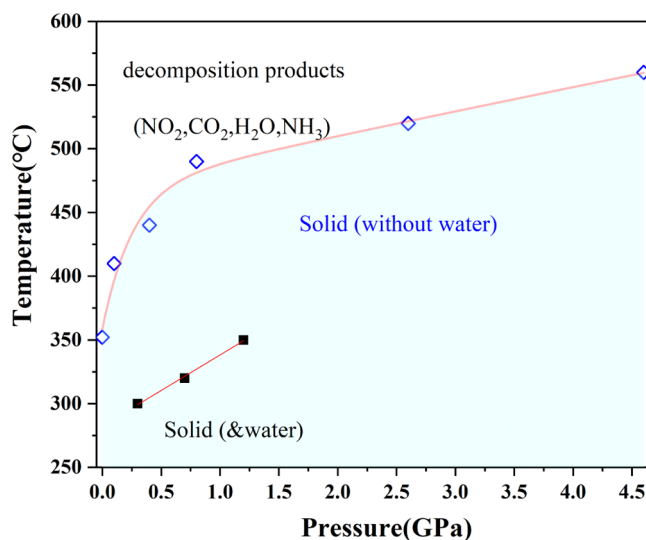

Figure 9. Decomposition/dissolution boundary of the LLM-105 crystal under high pressure with/without water.

and without water. In a previous work, we concluded that increasing pressure decelerates the thermal decay processes.[23] At a relatively low pressure (<1 GPa), high-temperature water can directly dissolve the organic crystals. From Raman peak shifts, 200 and 240 °C correspond to the initial soluble temperatures for LLM-105 crystals at the onset pressures of 0.3 and 0.7 GPa, respectively. Also, the decomposition temperatures are a little higher than the soluble temperatures when the initial pressure is below 1 GPa. From Raman spectra and microscopic images, the decomposition temperature is 300 °C at 0.3 GPa, while it is 320 °C with an initial pressure of 0.7 GPa. As a consequence, HP-HT water accelerates the thermal decay processes. From Figure 9, it is clear that the existence of HP-HT water reduced the decomposition temperature of the LLM-105 crystal to a large extent. This is because HP-HT water can act as a catalyst in the decomposition processes of LLM-105.

4. CONCLUSIONS
In conclusion, the interaction between LLM-105 and water under HP-HT was investigated. The dissolution behavior of LLM-105 in high-pressure and high-temperature water is related to the initial pressure. When the initial pressure is less than 1 GPa, LLM-105 crystals first dissolved in high-temperature water. For initial pressures above 1 GPa, LLM-105 particles only decompose in high-temperature water. At lower initial pressures, the LLM-105 sample particles can be completely dissolved in high-temperature water. The saturating solution facilely recrystallizes rodlike LLM-105 crystals for the large ratio of LLM-105 in the chamber. At higher pressures, the dissolving process is repressed and the sample decomposes with increasing temperature. In addition, the temperature−

pressure decomposition boundary of the water environment was established. The results reveal that the presence of water significantly lowered the LLM-105 crystal decomposition temperature. As a consequence, high-pressure high-temperature water can not only act as a solvent in the dissolving process but also act as a catalyst in the decomposing process. This work not only provides insights into the interaction between LLM-105 but also contributes to the response of energetic materials under extreme conditions and their practical applications in complex situations.

◼ ASSOCIATED CONTENT

ⓈⒾ Supporting Information

The Supporting Information is available free of charge at https://pubs.acs.org/doi/10.1021/acsomega.3c03107.

> Structure of the LLM-105 crystal (Figure S1), Raman and FITR spectra of LLM-105 (Figure S2), Raman spectra of LLM-105 crystals in water with the initial pressure of 0.7 GPa at 320 °C for different durations (Figure S3), Raman spectra and related Raman shifts of the LLM-105 crystals in water with the initial pressure of 0.3 GPa at different temperatures (Figure S4), ruby fluorescence spectra and temperature-dependent peak position of the ruby R1 line (Figure S5), temperature-dependent Raman spectra for the LLM-105 crystals in water with the initial pressure of 0.3 GPa (Figure S6), optical micrographs of LLM-105 crystals in high-temperature water at the initial pressure of 0.3 GPa (Figures S7 and S8), and decomposition boundary of the LLM-105 crystal under high pressure with/without water (Table S1) (PDF)

◼ AUTHOR INFORMATION

Corresponding Authors

Junke Wang − *Department of Physics, University of Science and Technology of China, Hefei 230026 Anhui, China*; Email: Wangjk11@mail.ustc.edu.cn

Xiaoyu Sun − *The Centre for Physical Experiments, University of Science and Technology of China, Hefei 230026 Anhui, China*; Email: xysun2015@ustc.edu.cn

Rucheng Dai − *The Centre for Physical Experiments, University of Science and Technology of China, Hefei 230026 Anhui, China*; Email: dairc@ustc.edu.cn

Zengming Zhang − *The Centre for Physical Experiments and Key Laboratory of Strongly Coupled Quantum Matter Physics, Chinese Academy of Sciences, School of Physical Sciences, University of Science and Technology of China, Hefei 230026 Anhui, China*; ⓞ orcid.org/0000-0001-8245-9955; Email: zzm@ustc.edu.cn

Authors

Chan Gao − *College of Mathematics and Physics, Chengdu University of Technology, Chengdu 610059 Sichuan, China*

Zilong Xu − *Department of Physics, University of Science and Technology of China, Hefei 230026 Anhui, China*

Di Mai − *Department of Physics, University of Science and Technology of China, Hefei 230026 Anhui, China*

Zhongping Wang − *The Centre for Physical Experiments, University of Science and Technology of China, Hefei 230026 Anhui, China*

Hongzhen Li − *Institute of Chemical Materials, China Academy of Engineering Physics, Mianyang 621900 Sichuan, China*; ⓞ orcid.org/0000-0002-8924-3417

Complete contact information is available at:
https://pubs.acs.org/10.1021/acsomega.3c03107

Notes

The authors declare no competing financial interest.

◼ ACKNOWLEDGMENTS

◼ REFERENCES

(1) Akiya, N.; Savage, P. E. Roles of Water for Chemical Reactions in High-Temperature Water. *Chem. Rev.* **2002**, *102*, 2725−2750.

(2) Fang, Z.; Fang, C. Complete Dissolution and Hydrolysis of Wood in Hot Water. *AIChE J.* **2008**, *54*, 2751−2758.

(3) Hashaikeh, R.; Fang, Z.; Butler, I. S.; Hawari, J.; Kozinski, J. A. Hydrothermal dissolution of willow in hot compressed water as a model for biomass conversion. *Fuel* **2007**, *86*, 1614−1622.

(4) Sasaki, M.; Fang, Z.; Fukushima, Y.; Adschiri, T.; Arai, K. Dissolution and hydrolysis of cellulose in subcritical and supercritical water. *Ind. Eng. Chem. Res.* **2000**, *39*, 2883−2890.

(5) Ogihara, Y.; Smith, R. L.; Inomata, H.; Arai, K. Direct observation of cellulose dissolution in subcritical and supercritical water over a wide range of water densities (550−1000 kg/m³). *Cellulose* **2005**, *12*, 595−606.

(6) Nagai, Y.; Smith, R. L.; Inomata, H.; Arai, K. Direct observation of polyvinylchloride degradation in water at temperatures up to 500 °C and at pressures up to 700 MPa. *J. Appl. Polym. Sci.* **2007**, *106*, 1075−1086.

(7) Fang, Z.; Smith, R. L.; Inomata, H.; Arai, K. Phase behavior and reaction of polyethylene terephthalate−water systems at pressures up to 173 MPa and temperatures up to 490 °C. *J. Supercrit. Fluids* **1999**, *15*, 229−243.

(8) Smith, R. L.; Fang, Z.; Inomata, H.; Arai, K. Phase behavior and reaction of nylon 6/6 in water at high temperatures and pressures. *J. Appl. Polym. Sci.* **2000**, *76*, 1062−1073.

(9) Wu, C. J.; Laurence, F. E.; Yang, L. H.; Goldman, N.; Bastea, S. Catalytic behavior of dense hot water. *Nat. Chem.* **2009**, *1*, 57−62.

(10) He, Z. H.; Chen, J.; Wu, Q.; Ji, G. F. Special catalytic effects of intermediate-water for rapid shock initiation of β-HMX. *RSC Adv.* **2016**, *6*, 93103−93110.

(11) Pagoria, P. F.; Mitchell, A. R.; Schmidt, R. D.; Simpson, R. L.; Garcia, F.; Forbes, J. W.; Swansiger, R.; Hoffman, D. M. *Synthesis, Scale-up, and Characterization of 2,6-Diamino-3,5-Dinitropyrazine-1-Oxide (LLM-105)*, Technical Report No. UCRL-JC-130518: Lawrence Livermore National Laboratory1998.

(12) Zhang, C.; Wang, X.; Huang, H. π-stacked interactions in explosive crystals: buffers against external mechanical stimuli. *J. Am. Chem. Soc.* **2008**, *130*, 8359−8365.

(13) Tarver, C. M.; Urtiew, P. A.; Tran, T. D. Sensitivity of 2,6-Diamino-3,5-Dinitropyrazine-1-Oxide. *J. Energ. Mater.* **2005**, *23*, 183−203.

(14) Xu, W.; An, C.; Wang, J.; Dong, J.; Geng, X. Preparation and properties of an insensitive booster explosive based on LLM-105. *Propellants, Explos., Pyrotech.* **2013**, *38*, 136−141.

(15) Gilardi, R. D.; Butcher, R. J. 2,6-Diamino-3,5-dinitro-1,4-pyrazine-1-oxide. *Acta Crystallogr., Sect. E: Struct. Rep. Online* **2001**, *57*, o657−o658.

(16) Manaa, M. R.; Kuo, I. F. W. L.; Fried, E. First-principles high pressure unreacted equation of state and heat of formation of crystal 2,6-diamino-3,5-dinitropyrazine-1-oxide (LLM-105). *J. Chem. Phys.* **2014**, *141*, No. 064702.

(17) Stavrou, E.; Riad Manaa, M.; Zaug, J. M.; Kuo, I. F. W.; Pagoria, P. F.; Kalkan, B.; Crowhurst, J. C.; Armstrong, M. R. The high pressure structure and equation of state of 2,6-diamino-3,5-dinitropyrazine-1-oxide (LLM-105) up to 20 GPa: X-ray diffraction measurements and first principles molecular dynamics simulations. *J. Chem. Phys.* **2015**, *143*, No. 144506.

(18) Ma, H. X.; Song, J. R.; Zhao, F. Q.; Gao, H. X.; Hu, Z. R. Crystal Structure, Safety Performance and Density-Functional Theoretical Investigation of 2,6-Diamino-3,5-Dinitropyrazine-1-Oxide (LLM-105). *Chin. J. Chem.* **2008**, *26*, 1997−2002.

(19) Williamson, D. M.; Gymer, S.; Taylor, N. E.; Walley, S. M.; Jardinea, A. P.; Glauserb, A.; Frenchb, S.; Wortleyb, S. Characterization of the impact response of energetic materials: observation of a low-level reaction in 2,6-diamino-3,5-dinitropyrazine-1-oxide (LLM-105). *RSC Adv.* **2016**, *6*, 27896−27900.

(20) Yuan, W. S.; Gan, Y. D.; Jiang, C. L.; Zhu, S. H.; Zhang, M. J.; Liu, F. S.; Tang, B.; Hong, D.; Liu, Q. J. First-principles calculations of the electronic, vibrational, and thermodynamic properties of 2,6-diamino-3,5-dinitropyrazine-1-oxide (LLM-105). *Chem. Phys.* **2021**, *548*, No. 111232.

(21) Zhang, C. Y.; Shu, Y. J.; Zhao, X. D.; Dong, H. S.; Wang, X. F. Theoretical studies on the reaction OH+CH3SiH2CH3. *J. Mol. Struct.: THEOCHEM* **2005**, *728*, 25−29.

(22) Gump, J. C.; Stoltz, C. A.; Mason, B. P.; Freedman, B. G.; Ball, J. R.; Peiris, S. M. Equations of state of 2,6-diamino-3,5-dinitropyrazine-1-oxide. *J. Appl. Phys.* **2011**, *110*, No. 073523.

(23) Xu, Z.; Su, H.; Zhou, X.; Wang, X.; Wang, J.; Gao, C.; Sun, X.; Dai, R.; Wang, Z.; Li, H.; Zhang, Z. Pressure- and Temperature-Dependent Structural Stability of LLM-105 Crystal. *J. Phys. Chem. C* **2019**, *123*, 1110−1119.

(24) Averkiev, B. B.; Antipin, M. Y.; Yudin, I. L.; Sheremetev, A. B. X-ray Structural Study of Three Derivatives of Dinitropyrazine. *J. Mol. Struct.* **2002**, *606*, 139−146.

(25) Gilardi, R. D.; Butcher, R. J. 2,6-Diamino-3,5-dinitro-1,4-pyrazine dimethyl sulfoxide solvate. *Acta Crystallogr., Sect. E: Struct. Rep. Online* **2001**, *57*, o757−o759.

(26) Zhou, X.; Shan, J.; Chen, D.; Li, H. Tuning the Crystal Habits of Organic Explosives by Antisolvent Crystallization: The Case Study of 2,6-dimaino-3,5-dinitropyrazine-1-oxid (LLM-105). *Crystals* **2019**, *9*, No. 392.

(27) Zhou, X.; Zhang, Q.; Xu, R.; Chen, D.; Hao, S.; Nie, F.; Li, H. A novel spherulitic self-assembly strategy for organic explosives: modifying the hydrogen bonds by polymeric additives in emulsion crystallization. *Cryst. Growth Des.* **2018**, *18*, 2417−2423.

(28) Wu, Q.; Yang, C.; Pan, Y.; Xiang, F.; Liu, Z.; Zhu, W.; Xiao, H. First-Principles Study of the Structural Transformation, Electronic structure, and Optical Properties of Crystalline 2,6-Diamino-3,5-Dinitropyrazine-1-Oxide under High Pressure. *J. Mol. Model.* **2013**, *19*, 5159−5170.

(29) Xiao, Q.; Sui, H.; Yu, Q.; Chen, J.; Yin, Y.; Ju, X. Gas Releasing Mechanism of LLM-105 Using Two-Dimensional Correlation Infrared Spectroscopy. *Propellants Explos. Pyrotech.* **2019**, *44*, 1375−1383.

(30) Lan, Q.; Zhang, H.; Ni, Y.; Chen, J.; Wang, H. Thermal decomposition mechanisms of LLM-105/HTPB plastic-bonded explosive: ReaxFF-lg molecular dynamics simulations. *J. Energ. Mater.* **2021**, *10*, No. 1968071.

(31) Yu, Q.; Zhao, C.; Liao, L.; Li, H.; Sui, H.; Yin, Y.; Li, J. A mechanism for two-step thermal decomposition of 2,6-diamino-3,5-dinitropyrazine-1-oxide (LLM-105). *Phys. Chem. Chem. Phys.* **2020**, *22*, 13729−13736.

(32) Wang, J.; Xiong, Y.; Li, H.; Zhang, C. Reversible Hydrogen Transfer as New Sensitivity Mechanism for Energetic Materials against External Stimuli: A Case of the Insensitive 2,6-Diamino-3,5-dinitropyrazine-1-oxide. *J. Phys. Chem. C* **2018**, *122*, 1109−1118.

(33) Wang, J.; Gao, C.; Xu, Z.; Zhong, C.; Dai, R.; Wang, Z.; Li, H.; Zhang, Z. Pressure effects on the thermal decomposition of the LLM-105 crystal. *Phys. Chem. Chem. Phys.* **2022**, *24*, 2396−2402.

(34) Mao, H. K.; Bell, P. M.; Shaner, J. W.; Steinberg, D. J. Specific volume measurements of Cu, Mo, Pd, and Ag and calibration of the ruby R1 fluorescence pressure gauge from 0.06 to 1 Mbar. *J. Appl. Phys.* **1978**, *49*, 3276−3283.

(35) Savage, P. E. Organic chemical reactions in supercritical water. *Chem. Rev.* **1999**, *99*, 603−621.

(36) Ding, Z. Y.; Frisch, M. A.; Li, L.; Gloyna, E. F. Catalytic oxidation in supercritical water. *Ind. Eng. Chem. Res.* **1996**, *35*, 3257−3279.

(37) Smith, I. Single-molecule catalysis. *Science* **2007**, *315*, 470−471.

(38) Vöhringer-Martinez, E.; Hansmann, B.; Hernandez, H.; Francisco, J. S.; Troe, J.; Abel, B. Water catalysis of a radical-molecule gas-phase reaction. *Science* **2007**, *315*, 497−501.

(39) Gao, C.; Wang, J.; Wang, J.; Dai, R.; Wang, Z.; Zhang, Z. Initial decomposition step and bimolecular hydrogen transfer of 3, 3′-diamino-4, 4′-azoxyfurazan under high pressure and high temperature. *Combust. Flame* **2022**, *140*, No. 111981.

(40) Qiu, L.; Li, Y.; Wang, Z.; Xue, M.; Xu, Z.; Meng, Z.; Ma, X.; Yi, D.; Lin, Z. Investigation of the Solubility of 3, 4-Diaminofurazan (DAF) and 3, 3′-Diamino-4, 4′-azoxyfurazan (DAAF) at Temperatures Between 293.15 K and 313.15 K. *Propellants, Explosives, Pyrotech.* **2016**, *41*, 883−887.